

# Sensitivity of short-range trio interactions to lateral relaxation of adatoms: Challenges for detailed lattice-gas modeling

Rajesh Sathiyarayanan, T.J. Stasevich<sup>1</sup>, T.L. Einstein\*

*Department of Physics, University of Maryland, College Park, Maryland 20742-4111, USA*

Received 29 November 2007; accepted for publication 18 January 2008

Available online 31 January 2008

## Abstract

Using ab-initio density functional theory, we have calculated the difference between A- and B-step formation energies on Pt(111) from orientation-dependent trio interactions. Our results show that the ratio of step formation energies is dependent on the local geometry and the lateral relaxation of the adatoms. The ratio approaches the experimentally observed values in the case of large supercells and wide adatom stripes, showing that use of a minimal lattice-gas model is inadequate for calculating step formation energies. Similar relaxation effects are seen in the step stiffness calculations from NN (nearest-neighbor) and NNN (next-nearest neighbor) interactions on Cu(100). To properly account for these effects within a lattice-gas framework and realign experiment with theory, we introduce a four adatom non-pairwise (quarto) interaction. For lattice-gas models involving multi-adatom direct interactions, the effects of lateral relaxations make delicate the parametrization of the characteristic energies.

© 2008 Elsevier B.V. All rights reserved.

**Keywords:** Density functional calculations; Lattice-gas models; Platinum; Copper; Surface structure, morphology, roughness, and topography; Low-index single-crystal surfaces; Stepped single-crystal surfaces; Lateral interactions

## 1. Introduction

Lattice-gas models are useful tools for categorizing structural properties, energetics and evolution of adatoms and steps on surfaces, allowing efficient statistical-mechanical calculations, as discussed in a variety of reviews [1–4]. The fundamental assumption is that all surface atoms sit in equivalent sites (or perhaps a handful of different types of sites), regardless of local geometry, and that lateral interactions then produce the local structure. Thus, the binding energy of a single species to this (high-symmetry) site is the strongest energy in the overlayer system. The second largest energy is the difference between binding to this favored site and to alternative sites. Then comes a hierarchy

of interaction energies for pairs of adsorbates in two favored sites, separated by various in-plane displacement vectors [3].

The simplest case, in which only nearest-neighbors are significant, corresponds to the popular bond-counting models of growth, particularly convenient because they naturally satisfy the detailed-balance criterion essential to Monte Carlo calculations of equilibrium and near-equilibrium properties [5]. Such models are a mainstay of much of our understanding of surface morphology and dynamics. They provide a valuable tool for including interparticle interactions in conceptual and numerical analyses.

In some cases, distant pairwise interactions also play an important role, and even multi-site interactions may be significant, especially when detailed accounting of phase boundaries or cluster shapes is sought [6–11]. The substrates in these studies are all mid or late transition or noble metals, where the electronic indirect interaction leads to rich behavior [3]. Since the Fermi level lies in the gap in semiconductors, there are no long-range oscillatory (Friedel) electronic inter-

\* Corresponding author. Fax: +1 301 314 9465.

E-mail address: [einstein@umd.edu](mailto:einstein@umd.edu) (T.L. Einstein).

URL: <http://www2.physics.umd.edu/~einstein/> (T.L. Einstein).

<sup>1</sup> Current address: Laboratory of Receptor Biology and Gene Expression, NCI, NIH, Bethesda, MD 20892, USA.

actions; any electronic interactions decay rapidly. There can be and often are long-range elastic/strain interactions on semiconductor surfaces, which do not fit neatly into a lattice-gas framework; in spite of the strong directionality of the covalent bonds underpinning semiconductors, reconstructions at surfaces often confound the use of lattice-gas models. Thus, there are relatively-few lattice-gas treatments of semiconductor surfaces, and they involve just short-range pair interactions [12–15].<sup>2</sup>

When the adsorbate–adsorbate interactions involve strong short-range lateral bonds (in particular, when direct bonding between such atoms is significant), it is possible (even likely) that the atoms can shift non-negligibly from their high-symmetry favored positions and cause subtle relaxation effects that can complicate the application of the lattice-gas framework. These effects seem to be especially significant for multi-site interactions, where the distortions are not along the bond direction.

The advent of powerful computer resources and of efficient, reliable, first-principles computational software has opened the door to calculating the total energy of periodic slabs containing enough atoms to allow one to extract the various lateral interactions of a lattice-gas model. Then these interactions are used in Monte Carlo to test whether they account adequately for experimental properties such as phase diagrams, equilibrium island shape, or step fluctuations. This field has become quite active [8–11]. Accordingly, it is timely to investigate what features might complicate that onerous task.

In this paper we discuss two important cases in which multi-site lattice-gas interactions are needed to describe overlayer properties but in which lateral relaxations hamper their evaluation [17]. One involves a new concept – orientation-dependent trio (three adatom non-pairwise) interactions – for determining the difference in energy per length between the two kinds of close-packed steps on a (111) fcc surface. Here we consider Pt(111), where this difference in energy is particularly large [18,19]. The second concerns how trio interactions affect models accounting for the stiffness anisotropy on {001} surfaces, focusing on Cu, for which extensive experimental data is available that sets limits on the ratios of the “effective” lattice-gas parameters. The role of lateral relaxations was noted long ago in an EAM (embedded atom method) calculation of the relative energies of linear and compact islands of Pt, Pd, and Ni on Pt(001) [20], with more emphasis on substrate lateral relaxations.

Our calculations use VASP (Vienna Ab-initio Simulation Package) [21,22], a widely-used state-of-the-art computational package based on density functional theory [23,24], that allow one to reliably compute the total energies of various configurations and extract there from these

interactions. They can in turn be used to calculate physical quantities such as step stiffness and step free energy, and the results can be compared with the experimental values.

## 2. Pt(111) – energy differences of close-packed steps

We recently used VASP to calculate, from a lattice-gas perspective, the difference in the free energies of A- and B-steps [(100) and (111) microfacets, respectively] on a Cu(111) surface. Normally in lattice-gas models, pairwise interactions alone are sufficient for computing key surface energies. However, pairwise interactions, no matter how long-range, do not distinguish between A- and B-steps. One must introduce other non-pairwise multi-site interactions involving at least three adatoms. As we also showed recently [25,26], an orientation-dependent trio (non-pairwise part of three adatom) interaction [3,27] of atoms forming an equilateral triangle with NN (nearest-neighbor) legs provides the most elementary way to account for the difference in step formation energies per NN spacing,  $E_A$  and  $E_B$ , of A- and B-steps, respectively. The ratio of the step formation energies ( $E_A/E_B$ ) was found to be 1.04. This is in good agreement with the experimentally measured values [28]. However, this case did not provide compelling evidence of the role of orientation-dependent trio interactions since  $E_A/E_B$  is so close to unity.

Here we consider a sterner test by examining orientation-dependent trio interactions on Pt(111), where the difference (both absolute and fractional) in A- and B-step formation energies is larger [18] than it is on Cu(111): specifically, the ratio of free energies at 625 K (i.e., the finite-temperature generalization of  $E_A/E_B$ ) is  $1.15 \pm 0.03$ . We find that the trio interactions, unlike their pairwise counterparts, are very sensitive to the lateral relaxation of adatoms.

Our VASP calculations of step formation energies used its ultrasoft pseudopotentials for Pt (with a plane wave cut-off of 14.1 Ryd.) and the Ceperley–Alder local density approximation (LDA) [29] (we used LDA because Boisvert et al. [30] showed that LDA produces a better estimate of the Pt surface energies than the generalized gradient approximation (GGA) [29]). The lattice parameter for Pt was determined to be 3.91 Å from a bulk LDA calculation using a  $1 \times 1 \times 1$  supercell with a  $13 \times 13 \times 13$  k-point grid (if we use GGA this distance is 3.99 Å).

Our straightforward calculation of the trio interaction energies for the isolated trimer on Pt(111) used a  $3 \times 3 \times 1$  k-point grid, a  $(4 \times 4 \times 14)$  supercell, and a slab of five atomic layers,<sup>3</sup> with the remainder as vacuum. We

<sup>3</sup> Increasing the slab thickness to seven atomic layers changes the quantitative results by perhaps 10% but not the semiquantitative behavior: e.g., in an early check of the “Trimer, min cell” configuration of Fig. 3a, we found that this increased thickness changes  $\Delta E_{AB}$  from  $-38$  to  $-34$  meV/atom. Since our goal has been to understand the role of relaxations rather than to compute the best possible estimate of  $\Delta E_{AB}$ , we opted for five layer slabs, saving a factor of two in run time. Note also that another early check showed that using GGA rather than LDA for the seven layer slab changed  $\Delta E_{AB}$  to  $-31$  meV/atom.

<sup>2</sup> Even the “corner” energy for kinks on steps on vicinal Si(100) [16] can be ascribed to attractive NNN interactions. Scant attention has been paid to possible multi-site terms and how they come into play in the saturation of dangling bonds.

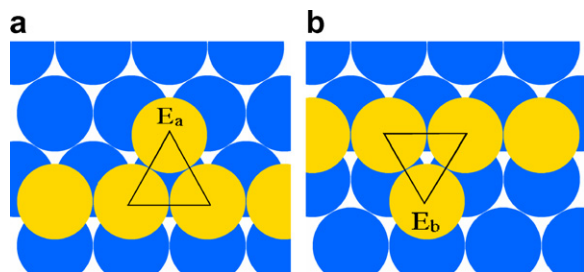


Fig. 1. Adatom trios on (111) surface (lighter (mustard) circles represent adatoms, darker (blue) circles represent substrate atoms) (a) A-trios have a substrate atom at their center (b) B-trios do not have a substrate atom at their center. All figures look down, normal to the surface plane, called  $\hat{z}$ . (For interpretation of the references to colour in this figure legend, the reader is referred to the web version of this article.)

placed three adatoms on both the top and the bottom of the slab so that any charge-transfer effects in computed energies cancel [31]. The adatoms were sited so that they formed either an A-trio ( $E_a$ ) or a B-trio ( $E_b$ ) (cf. Fig. 1). The middle layer was frozen to bulk positions, and all the other layers were allowed to relax in all directions until the net force on the atoms was less than  $0.01 \text{ eV}/\text{\AA}$  [32]. The difference between step formation energies are calculated from the trio interaction energies [26]:

$$\Delta E_{AB} \equiv E_A - E_B = \frac{1}{3}(E_a - E_b) \quad (1)$$

The results of these calculations,  $+6 \text{ meV/atom}$ , show that the formation energy  $E_B$  is smaller than  $E_A$ , consistent with the cited experimental results of Michely and Comsa [18], but with a magnitude only  $1/8$  that reported in the density functional calculations of Feibelman [19], who used an  $(8 \times 8 \times 4)$  substrate with 28 adatoms on one side.

To predict confidently the magnitude of multi-site interactions, it is important to understand the origin of this large difference between these two calculations. If we allow no relaxation (fixing atoms at the positions predicted by the continuation of bulk lattice structure), we find, remarkably, that for both the “Isolated trimer” and the “Feibelman” configurations  $E_A - E_B$  becomes negative, with values  $-40$  and  $-23 \text{ meV/atom}$ , respectively (see Fig. 2). Thus, relaxation<sup>4</sup> plays a crucial role in obtaining the (correct) sign of  $E_A - E_B$ , but also the large difference in strength. The triad in our elementary cell is isolated, while in Feibelman’s there are many neighbors.

Relaxations can be purely vertical (normal to the slab, i.e., along  $\hat{z}$ ) or more generally can also involve lateral displacements perpendicular to the normal. Our evidence shows that such lateral relaxations are crucial in determining the multi-site interactions accurately. If we allow only

<sup>4</sup> A quick calculation shows that lateral relaxations are more significant for Pt(111) than for Cu(111). For a strip of overlayer atoms four atoms wide, we compared the relaxation – inward – of the A- and B-edges. For Cu these lateral relaxations were  $0.051$  and  $0.070 \text{ \AA}$ , respectively (ratio = 1.37); for Pt they were about three times as large,  $0.124$  and  $0.204 \text{ \AA}$ , respectively (ratio = 1.645).

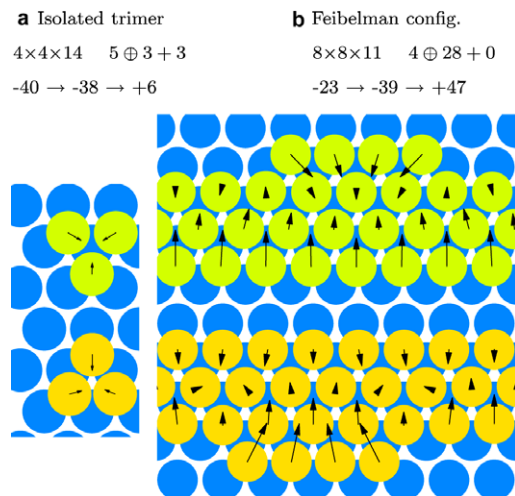


Fig. 2. Illustration of a basic isolated trio and the large structure used by Feibelman [19]. Beneath each descriptor is the size of the supercell ( $n_x \times n_y \times n_z$ ) and the layer structure (# full atomic layers  $\oplus$  # adatoms on top of slab + # atoms beneath). In the third row are tabulated the difference  $E_A - E_B$  in meV per adatom with no relaxation  $\rightarrow$  the comparable energy when only vertical relaxation is allowed  $\rightarrow$  the comparable energy when lateral relaxation is allowed also. In the figure panels the arrows show the magnitude – amplified tenfold for clarity – and direction of the lateral relaxation. For compactness, each panel combines a pair of configurations onto a single lattice. The upper configuration (lime atoms) depicts an A-step while the lower (mustard atoms) shows a B-step. For specificity in discussions, the vertical direction in the figure is called  $\hat{y}$  and the horizontal  $\hat{x}$ , with  $\hat{z}$  the normal to the slab as in Fig. 1. See text for discussion.

vertical relaxations, there is little difference (about  $0.01 \text{ \AA}$ ) in the vertical positions of the two trios (although the vertical (inward) relaxation of each is an order of magnitude larger). More significantly, purely vertical relaxation only exacerbates the problem with  $\Delta E_{AB}$ , as we explicate in our study a sequence of intermediate configurations – illustrated in Fig. 3 – interpolating between the isolated trio case and Feibelman’s large-cell case, in which there are several “edge-atoms” (atoms bound to the edge), depicted in Fig. 2.

The illustrations show with arrows the lateral displacements, magnified by a factor of ten in size for clarity, of the adatoms. As mentioned, these in-plane displacements are crucial in accounting for the difference of the energies of A- and B-steps. When only vertical relaxation is allowed, we get the intermediate energies in the third row of tabulated information in the figures. In all cases,  $\Delta E_{AB}$  remains – unphysically – negative, as for the completely unrelaxed calculation. Except for the isolated triad, the magnitude actually increases, typically by at least 50%, making the discrepancy from experiment worse.

For a simple triad of adatoms in a minimum-size supercell (cf. Fig. 3a), the formation energy  $E_B$  remains larger than  $E_A$ , with a larger difference than in the unrelaxed case. In this case, we also see that the lateral relaxations of the two orientations are about the same. In contrast, Fig. 2b shows that the lateral relaxations at the B-step are notably greater than those at the A-step. This behavior supports

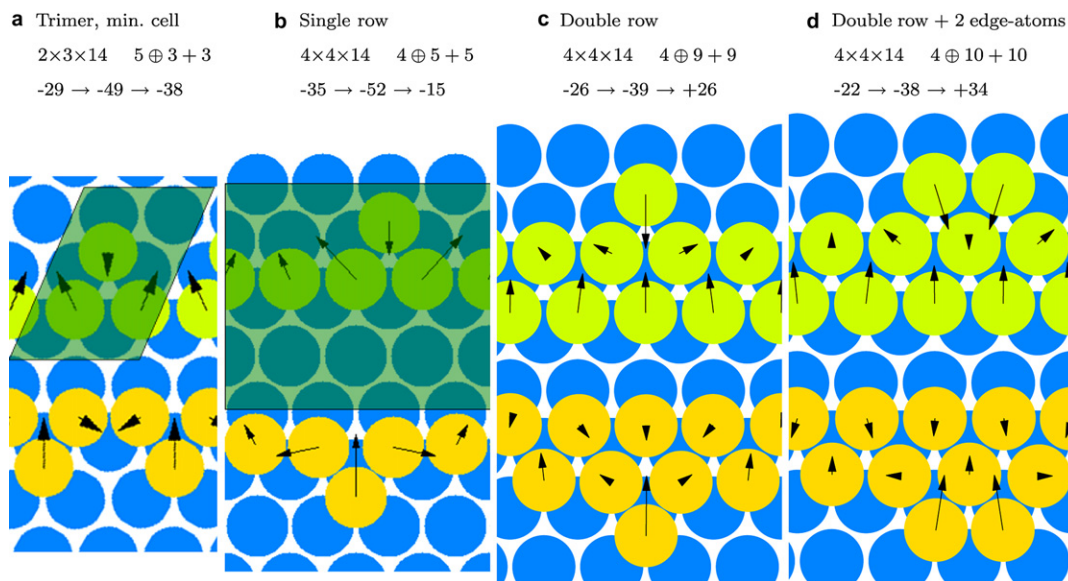


Fig. 3. Illustration of intermediate configurations considered in this study, progressing from an atom on a chain to larger structures leading towards Feibelman's configuration. Same notation as in Fig. 2. The shaded rhomboid in the upper part of panel (a) illustrates the 2D unit cell for this case. The corresponding shaded rectangle in panel (b) the larger size unit cell used in it and panels (c) and (d).

the idea that the energy lowering due to lateral relaxation is greater at the B-step than at the A-step, underpinning the positive value of  $\Delta E_{AB}$  in the experiment.

We chose the intermediate configurations to examine how the lateral relaxation depends on the lateral depth of the overlayer (the number of horizontal stripes used to represent the island or upper terrace) and on the interaction between adjacent edge-atoms. From another perspective, the latter can be viewed as interactions between the kink and antikink that define the beginning and end of the edge-atom grouping along an edge. Except for the minimal triad of panel a, each intermediate configuration was studied with  $(4 \times 4 \times 14)$ , five layer-thick supercells; edge-atoms were placed on the A-step edge or B-step edge (i.e., edge-atoms were added to these stripes to create either A-kink–antikink pairs on an A-step, each consisting of a B-link, or B-kinks).

In decomposing the energies for all six upper configurations, we note that the additional edge-atoms increase the total energy (per repeat length along  $\hat{x}$ ) by  $E_A$ <sup>5</sup> plus the number of edge-atoms times the energy of an atom in the close-packed interior of the overlayer [33]. The straight and edge-atom-decorated configurations are viewed as having the same edge energies. Similarly, for the lower configurations the difference per repeat length is raised by  $E_B$  plus the number of edge-atoms time the same 2D-bulk contribution. Thus,  $\Delta E_{AB}$  is just the difference in energy per repeat length of the total energy of the upper configuration and the lower one for each pair. The results are listed in the bottom row of the tabulation in Fig. 3.

<sup>5</sup> The kink and the antikink each add  $E_A$  but the overall length of the A-step is decreased by one link, subtracting  $E_A$ ; hence, a net increase by  $E_A$ .

For edge-atoms on a one adatom-wide stripe (Fig. 3b), the formation energy of B-steps was found to be greater than that of A-steps, similar to results with the  $(2 \times 3 \times 14)$  cell (Fig. 3a), but slightly reduced. This similarity is reflected in the adatom relaxations, as Fig. 3a and b shows. There is a repulsion between an edge-atom and its periodicity-replicated “images” due to the evident frustration of relaxation, especially along  $\hat{x}$ , in the stripe in Fig. 3a compared to Fig. 3b; furthermore, the relaxation along  $\hat{y}$  of the edge-atom is larger in Fig. 3b.<sup>6</sup> As we move across the series, the relaxations are stabilized as the overlayer structure becomes larger, and we see more clearly the asymmetry in the relaxations around edge-atoms on the two types of close-packed steps.

For kinks on two adatom-wide stripes (Fig. 3c and d), the step formation energy of A-steps is greater than that of B-steps, in agreement with previous theory and experiment and similar to results using the  $(8 \times 8 \times 11)$  supercell. Evidently, this is due to the lateral relaxations since this inequality does not hold for frozen structures or purely vertical relaxation. The addition of a row of adatoms changed  $\Delta E_{AB}$  by 40 meV/atom.

When there are two edge-atoms per cell (Fig. 3d), symmetry no longer constrains the lateral relaxation to lie along  $\hat{y}$ . Indeed, we see that the edge-atoms evidently attract each other modestly. This behavior can be understood from bond-energy–bond-order (BEBO) [34] arguments, since the edge-atoms have the fewest lateral neighbors. It

<sup>6</sup> Since the periodic boundary conditions produce edge-atoms that are separated by four atomic distances (as compared to two on  $(2 \times 3 \times 14)$  supercells), the difference between results gauges the strength of the repulsive interaction between edge-atoms. The difference of these differences for A- and B-steps makes a contribution of 20 meV to  $\Delta E_{AB}$ .

can also be described in terms of electrostatic attractions of the positively-charged edge-atoms at each end of a grouping [35,36]. Comparing Figs. 3d and 2b, we see that this horizontal relaxation of end of edge-atoms becomes greater for longer chains. This attraction between edge-atoms, which favors the formation of a nascent chain along the step edge, can be recast as a repulsion between the kink and the antikink bounding the minichain.<sup>7</sup> Inspection of the upper and lower parts of Fig. 3d shows that the  $\hat{x}$  component of relaxation is rather similar; correspondingly, the change in  $\Delta E_{AB}$  from Fig. 3c is relatively modest; the major source of the change in  $\Delta E_{AB}$  comes from the greater inward (along  $\hat{y}$ ) relaxation at the B- vs. the A-step, as seen most clearly in Fig. 3c. Fig. 2b shows somewhat greater disparity in the magnitude of relaxation along  $\hat{y}$ , leading to a larger value of  $\Delta E_{AB}$ .

In summary, we find that the multi-site trio interactions are particularly sensitive to the lateral relaxation of the adatoms, which are in turn dependent on the size and local geometry of supercells used to calculate them. This raises questions as to the applicability of a simple lattice-gas description of these interactions, which necessarily assumes the adatoms sit in well-defined, high-symmetry positions.

### 3. Cu(100) – step stiffness anisotropy

We next consider the strain/relaxation-related effects on calculated trio interaction energies on Cu(100). Dieluweit et al. [37] showed that the NN Ising model cannot explain the experimentally observed step stiffness anisotropy. Based on a crude calculation, Zandvliet et al. [38,39] proposed that an attractive NNN interaction  $E_2 < 0$  could account for the discrepancy. With a fuller calculation using the solid-on-solid (SOS) approximation, some of us [40] showed that the effect of NNN attractions was even somewhat larger than they had predicted. However, the picture could be clouded by the existence of significant repulsive trio interactions. The strongest interaction is likely to originate from a configuration with the smallest perimeter [27], for this case a right-isosceles configuration with a pair of NN legs and an NNN hypotenuse. The SOS calculation shows that one then has an effective NNN interaction ( $\epsilon_2$ ), written as the sum of two components, illustrated in Fig. 4a:

$$\epsilon_2 = E_2 + E_d \quad (2)$$

<sup>7</sup> For large edge-atom chains, we expect that the  $\hat{x}$  relaxation is significant only for edge-atoms near either end of the chain. Though this would seem at first glance to then amount to a negligible finite-size correction, the prescription, described above, for computing the step energies subtracts the energies of the edge-atoms nearer the middle of the chains from those of an edge without edge-atoms, so that the values at the ends continue to be emphasized. While this feature turns out not to be crucial in the present problem, it could in principle confound straightforward assessment of step energies.

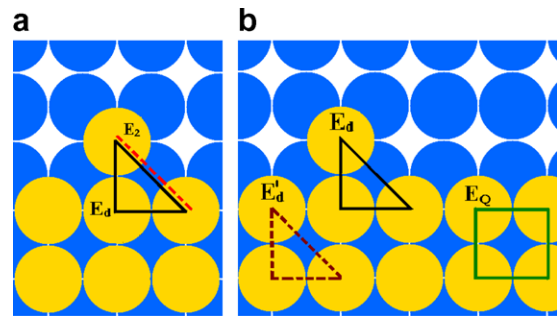


Fig. 4. (a) Effective NNN interactions on a (100) surface. (b) Multi-site interactions  $E_d$  (solid triangle),  $E'_d$  (broken triangle) and  $E_Q$  (square). The trio  $E_d$  has adatoms on the step edge whereas  $E'_d$  has no adatoms on the step edge.

To investigate whether the parameters deduced from such statistical–mechanical fits to anisotropies correspond to actual atomistic energies, we used VASP to calculate these interactions [26]. We computed the energies of eight different ordered overlayer superlattices (depicted in Fig. 2 of Ref. [26]) and fit with an adsorption energy, three pair interactions ( $E_1$ ,  $E_2$  and a third NN  $E_3$ ), and two trios (an isosceles-right triangle, with  $E_1$  and  $E_2$  legs, and collinear, with two  $E_1$  and one  $E_3$  legs). Consistent with the above scenario,  $E_3$  was negligible, and the collinear trio configuration had much smaller magnitude than  $E_d$ . We found  $E_1 = -332 \pm 16$  meV and  $E_2 = -47 \pm 9$  meV, yielding  $E_2/E_1 \approx \frac{1}{7}$ , consistent with the modeling of the data. However,  $E_d = 52 \pm 12$  meV, roughly cancelling  $E_2$  and so leading to essentially a NN Ising model, known to be inadequate.

To check whether relaxation effects played a role in this conundrum, we revisited the problem, using the same approach and parameters as in Ref. [26] but with a bigger supercell ( $4 \times 4 \times 14$ ). As shown in Fig. 4b, we distinguished two types of NN right-isosceles trios, one in the dense interior of a  $(1 \times 1)$  overlayer, where symmetry precludes significant lateral relaxation, and another at the edge, with one or two of the three some of atoms being edge-atoms with just one or two (lateral) NN bonds.

Since the local geometry of these adatoms differ, we could anticipate that the associated trio interaction energies would also differ. This is based on the idea that the isosceles-right trio adatoms ( $E'_d$ ) inside a stripe cannot relax laterally as much as the trios with vertices on the step ( $E_d$ ). This reasoning leads to the prediction – which proves accurate – that  $E_d$  should be less repulsive than  $E'_d$ . The trio energy calculated by us earlier corresponds to a linear combination of  $E_d$  and  $E'_d$ , weighted more dominantly by  $E'_d$ . However, the calculation of the step stiffness depends on broken step edge trios, which necessarily correspond to  $E_d$ . To distinguish these two trios here, we calculated the energies of four different adatom configurations,<sup>8</sup> and we

<sup>8</sup> Fig. 2 of Ref. [26] shows two configurations, the right most panels in the middle and bottom rows. In addition, there are configurations with extra atoms next to full rows.

solved the resultant linear system of equations. With this correction, the step edge isosceles-right trio interaction becomes:

$$E_d \approx 12.5 \pm 0.5 \text{ meV} \quad (3)$$

because the increased lateral relaxation decreases the repulsion between the three nearby atoms with little ( $\sim 9$  meV) change to the pair interactions. Now the effective NNN interaction is

$$\epsilon_2 = E_2 + E_d \approx -34 \text{ meV} \quad (4)$$

The ratio of this effective NNN interaction to the effective NN interaction  $\epsilon_1 = E_1 + 2E_d$  is

$$\epsilon_2/\epsilon_1 \sim \frac{1}{9} \quad (5)$$

which is much closer to experimental expectations.

Distinguishing between the step edge trio interactions  $E_d$  and those in the interior (2D-bulk)  $E'_d$  is inconsistent with a proper lattice-gas picture, where interactions should not depend on local position and geometry. We can remedy this problem by introducing a four adatom, non-pairwise and non-trio “quarto” interaction (the possibility of such interactions has been known for over three decades [3,41], but to the best of our knowledge, it has been invoked only once in an actual calculation of adsorbate energetics [42]). This quarto interaction distinguishes between the two trios because it is present only for 2D-bulk trios  $E'_d$ :

$$E'_d = E_d + \frac{3}{4}E_Q \quad (6)$$

Since this quarto interaction acts to reconfine the adatoms to their laterally unrelaxed positions, we expect it to be repulsive and rather substantial in magnitude. Indeed, we find for Cu(001) that the quarto interaction has value  $E_Q = 53 \pm 16$  meV. This is a significant energy, e.g., in comparison to the collinear trio  $E_c = -15$  meV and third NN interaction  $E_3 = -8$  meV [40]. Hence,  $E_Q$  is likely to have consequences in calculations of other properties. This formulation, while somewhat awkward in replacing  $E'_d$  by the weaker  $E_d$  as the relevant trio energy, does provide a viable and consistent way to bridge the theoretical step stiffness with experimental measurements on Cu(100).

#### 4. Conclusion

Within a lattice-gas framework, we have shown that the inclusion of an orientation-dependent trio interaction can account for the difference in A- and B-step formation energies on Pt(111). When calculating trio interactions from first-principles, however, care must be taken. As reported here, these interactions can be exquisitely sensitive to the geometry and structure of the supercell used to calculate them. Such sensitivity to local relaxation can complicate a simple lattice-gas description. It is the trio interaction for sites involving edge-atoms that accounts for the difference in energy of the A- and B-steps. These trio repulsions

are significantly weaker, due to lateral relaxations, than the apparent energy of trios in the interior (“bulk”) of the surface. However, the idea of a position-dependent interaction is inconsistent with the lattice-gas formalism. On a square lattice we can account for the relaxation of trios near step edges by introducing a non-pairwise quarto interaction  $E_Q$  among four neighboring adatoms. Such an interaction can bridge the theoretical step stiffness with experimental measurements on Cu(100). In that case, we find what amounts to a relatively large, repulsive quarto interaction  $E_Q \approx 0.05$ eV that has significant physical consequences in our problem and presumably more generally (note, however, that quarto interactions are unlikely to play a role in the energy difference between A- and B-steps for (111) surfaces, since the obvious compact configurations contain one *a* and one *b* triad).

These subtleties in homoepitaxial systems involve configurations in which atoms adsorb at (lateral) nearest-neighbor sites. In such cases the direct interaction between the atoms in the uppermost layer play a significant, usually predominant role; they are strong enough to move atoms significantly from high-symmetry positions. In particular, BEBO [34] arguments predict that the bond lengths will decrease near edges in a way that compensates for the loss of nearest-neighbors. For configurations that involve atoms sufficiently distant (usually second-neighbor or beyond) that the indirect, through-substrate interaction accounts overwhelmingly for the lateral interaction, such relaxation effects should be insignificant. Likewise, for heteroepitaxy in which the adatoms are much smaller than the substrate atoms, the direct interaction is likely to be unimportant even for nearest-neighbors. Remarkably, the effects are more significant for multi-adatom interactions than for pair interactions, presumably because in the latter case symmetry typically dictates that lateral relaxations must occur along the bond direction; for homoepitaxy, such “longitudinal” relaxations are likely to be relatively costly energetically (it would be interesting to examine this problem for heteroepitaxy in the case of small mismatch).

The effects of lateral relaxations on short-range interactions of overlayer atoms can be expected to be even more important on open surfaces, so long as the adatoms are still close enough to experience direct interactions. Indeed, such issues have been noticed in calculations for {110} surfaces of two fcc metals: Al [10] and Cu [43].

This research provides a stark warning about blithely applying multi-interaction lattice-gas models to overlayer systems involving adatoms having size comparable to the substrate atoms and residing in structures with nearest-neighbor occupation. We find then that the appropriate trio interactions for determining one sort of statistical property can differ from that needed to assessing another. Resorting to interactions among four or more adatoms to “correct” for the relaxations lowering trio interactions is disquieting. Given the fundamental place of the lattice-gas picture in modeling behavior, it is important to find a way to go beyond ad hoc patches. Progress calls for imag-

inative reformulations of the overlayer problem, and it is heartening that some are already appearing [44]. The goal should be to provide a systematic approach to parametrize the lattice-gas model for targeted applications in a way that takes into account the subtle effects of lateral relaxations on direct interactions.

### Acknowledgments

This work was supported by the University of Maryland NSF-MRSEC, Grant No. DMR 05-20471, with partial support from DOE CMSN grant DEFG0205ER46227. Computational support for VASP calculations was provided by National Computational Science Alliance at University of Illinois, Urbana Champaign. We thank Peter Feibelman for sharing his VASP files with us and Kristen Fichthorn for several fruitful interactions.

### References

- [1] L.D. Roelofs, in: R. Vanselow, R.F. Howe (Eds.), *Chemistry and Physics of Solid Surfaces IV*, Springer, Berlin, 1982 (Chapter 10).
- [2] B.N.J. Persson, *Surf. Sci. Rep.* 15 (1992) 1.
- [3] T.L. Einstein, in: W.N. Unertl (Ed.), *Physical Structure of Solid Surfaces, Handbook of Surface Science*, vol. 1, Elsevier, Amsterdam, 1996, p. 577.
- [4] A. Patrykiewicz, S. Sokolowski, K. Binder, *Surf. Sci. Rep.* 37 (2000) 207.
- [5] M.E.J. Newman, G.T. Barkema, *Monte Carlo Methods in Statistical Physics*, Oxford University Press, 1999.
- [6] S.-J. Koh, G. Ehrlich, *Phys. Rev. B* 60 (1999) 5981.
- [7] L. Österlund, M.Ø. Pedersen, I. Stensgaard, E. Lægsgaard, F. Besenbacher, *Phys. Rev. Lett.* 83 (1999) 4812.
- [8] C. Stampfl, *Catal. Today* 105 (2005) 17; M. Borg et al., *Chem. Phys. Chem.* 6 (2005) 1923.
- [9] Y. Zhang, V. Blum, K. Reuter, *Phys. Rev. B* 75 (2007) 235406.
- [10] Y. Tiwary, K.A. Fichthorn, *Phys. Rev. B* 75 (2007) 235451.
- [11] C. Lazo, F.J. Keil, Preprint and Seminar at North Carolina State U., 2007.
- [12] N. Akutsu, Y. Akutsu, *Surf. Sci.* 376 (1997) 92; N. Akutsu, Y. Akutsu, *J. Phys.: Condens. Matter* 11 (1999) 6635.
- [13] V.P. LaBella, D.W. Bullock, M. Anser, Z. Ding, C. Emery, L. Bellaiche, P.M. Thibado, *Phys. Rev. Lett.* 84 (2000) 4152.
- [14] M. Biehl, M. Ahr, W. Kinzel, M. Sokolowski, T. Volkmann, *Europhys. Lett.* 53 (2001) 169.
- [15] M.A. Albao, D.-J. Liu, M.S. Gordon, J.W. Evans, *Phys. Rev. B* 72 (2005) 195420.
- [16] B.S. Swartzentruber, Y.-W. Mo, R. Kariotis, M.G. Lagally, M.B. Webb, *Phys. Rev. Lett.* 65 (1990) 1913.
- [17] T.L. Einstein, R. Sathiyarayanan, T.J. Stasevich, <<http://meetings.aps.org/link/BAPS.2007.MAR.H42.10>>.
- [18] Th. Michely, G. Comsa, *Surf. Sci.* 256 (1991) 217.
- [19] P.J. Feibelman, *Surf. Sci.* 463 (2000) L661.
- [20] A.F. Wright, M.S. Daw, C.Y. Fong, *Phys. Rev. B* 42 (1990) 9409.
- [21] G. Kresse, J. Hafner, *Phys. Rev. B* 47 (1993) R558; G. Kresse, J. Hafner, *Phys. Rev. B* 49 (1994) 14251.
- [22] G. Kresse, J. Furthmüller, *Comput. Mater. Sci.* 6 (1996) 15; G. Kresse, J. Furthmüller, *Phys. Rev. B* 54 (1996) 11169.
- [23] P. Hohenberg, W. Kohn, *Phys. Rev.* 136 (1964) B864.
- [24] W. Kohn, L.J. Sham, *Phys. Rev.* 140 (1965) A1133.
- [25] T.J. Stasevich, H. Gebremariam, T.L. Einstein, M. Giesen, C. Steimer, H. Ibach, *Phys. Rev. B* 71 (2005) 245414.
- [26] T.J. Stasevich, T.L. Einstein, S. Stolbov, *Phys. Rev. B* 73 (2006) 115426.
- [27] T.L. Einstein, *Langmuir* 7 (1991) 2520.
- [28] M. Giesen, *Prog. Surf. Sci.* 68 (2001) 1.
- [29] J.P. Perdew, in: P. Ziesche, H. Eschrig (Eds.), *Electronic Structure Theory of Solids*, Akademie Verlag, Berlin, 1991; J.P. Perdew, J.A. Chevary, S.H. Vosko, K.A. Jackson, M.R. Pederson, D.J. Singh, C. Fiolhais, *Phys. Rev. B* 46 (1992) 6671.
- [30] G. Boisvert, L.J. Lewis, M. Scheffler, *Phys. Rev. B* 57 (1998) 1881.
- [31] K.A. Fichthorn, M. Scheffler, *Phys. Rev. Lett.* 84 (2000) 5371; K.A. Fichthorn, M.L. Merrick, M. Scheffler, *Phys. Rev. B* 68 (2003) 041404(R).
- [32] M. Methfessel, A.T. Paxton, *Phys. Rev. B* 40 (1989) 3616.
- [33] R.C. Nelson, T.L. Einstein, S.V. Khare, P.J. Rous, *Surf. Sci.* 295 (1993) 462.
- [34] H.S. Johnston, C. Parr, *J. Am. Chem. Soc.* 85 (1963) 2544.
- [35] R. Smoluchowski, *Phys. Rev.* 60 (1941) 661.
- [36] P. Jiang, F. Jona, P.M. Marcus, *Phys. Rev. B* 35 (1987) 7952.
- [37] S. Dieluwit, H. Ibach, M. Giesen, T.L. Einstein, *Phys. Rev. B* 67 (2003) 121410(R).
- [38] R. Van Moere, H.J.W. Zandvliet, B. Poelsema, *Phys. Rev. B* 67 (2003) 193407.
- [39] H.J.W. Zandvliet, R. Van Moere, B. Poelsema, *Phys. Rev. B* 68 (2003) 073404.
- [40] T.J. Stasevich, T.L. Einstein, R.K.P. Zia, M. Giesen, H. Ibach, F. Szalma, *Phys. Rev. B* 70 (2004) 245404.
- [41] W.A. Harrison, *Phys. Rev. B* 7 (1973) 2408.
- [42] L.D. Roelofs, S.M. Foiles, M.S. Daw, M.I. Baskes, *Surf. Sci.* 234 (1990) 63.
- [43] S. Vaikuntanathan, R. Sathiyarayanan, T.L. Einstein, unpublished.
- [44] Y. Tiwary, K.A. Fichthorn, *Bull. Am. Phys. Soc.* 53 (2008) abstract B20.00004, submitted for publication.